

THE WOODLAND BEACH CORE, DELAWARE: PALEOCENE-EOCENE RECORD OF A
MID-ATLANTIC SHORELINE SEQUENCE

by

Matthew Smith
A Thesis
Submitted to the
Graduate Faculty
of
George Mason University
in Partial Fulfillment of
The Requirements for the Degree
of
Master of Science
Earth Systems Science

Committee:

Dr. Linda Hinnov, Thesis Director

Dr. Stacey Verardo, Committee Member

Dr. John J. Qu, Committee Member

Dr. James L. Kinter III, Department
Chair

Dr. Donna M. Fox, Associate Dean,
Office of Student Affairs & Special
Programs, College of Science

Dr. Peggy Agouris, Dean, College of
Science

Date: _____

Spring Semester 2019
George Mason University
Fairfax, VA

The Woodland Beach Core, Delaware: Paleocene-Eocene Record of a Mid-Atlantic
Shoreline Sequence

A thesis submitted in partial fulfillment of the requirements for the degree of Master of
Science at George Mason University

By

Matthew T. Smith
Bachelor of Science
University of Louisiana, 2014

Director: Linda Hinnov, Professor of Geology
Department of Atmospheric, Oceanic, and Earth Sciences

Spring Semester 2019
George Mason University
Fairfax, VA

Copyright 2019 Matthew Smith

All Rights Reserved

Acknowledgments

I would like to thank Dr. Peter McLaughlin of the Delaware Geological Survey for proposing the Woodland Beach core project and providing his support, expertise and access to the core. Thanks go also to the United States Geological Survey (USGS) for the internship during Summer 2017 to work on Woodland Beach core materials, and providing advice and use of equipment. Thanks go especially to Dr. Marci Robinson and Dr. Jean Self-Trail of the USGS for their expertise and advice on PETM foraminifera and calcareous nannofossils that they identified in the Woodland Beach core. Finally, I would like to thank my thesis committee members Dr. Stacey Verardo, Dr. John J. Qu, and especially my advisor Dr. Linda Hinnov for all their feedback and encouragement.

Table of Contents

	Page
List of Tables.....	v
List of Figures.....	vi
Abstract.....	vii
1. Introduction.....	1
2. Data.....	6
2.1 Geological setting.....	6
2.2 The Woodland Beach core.....	8
2.3 Well Logs.....	10
2.4 Foraminifera and Calcareous Nannofossils.....	13
2.5 RGB intensity scans of core photographs.....	14
3. Methods.....	17
3.1 Core sampling.....	17
3.2 Sample preparation for foraminifera.....	18
3.3 Time series methods.....	19
3.4 Artifacts: estimation and removal.....	21
4. Results.....	23
4.1 Benthonic and planktonic foraminifera count.....	23
4.2 Percent sand record.....	24
4.3 Spectral analysis of the residual red intensity series.....	27
5. Discussion.....	29
5.1 A preliminary biostratigraphy for Woodland Beach core.....	29
5.2 Evidence for variable sea levels in the early Eocene.....	30
5.3 An Interpretation of Milankovitch cycles.....	32
6. Conclusions.....	35
Appendix.....	39
List of References.....	42
Biography.....	45

List of Tables

	Page
Table 1.....	25

List of Figures

	Page
Figure 1.....	3
Figure 2.....	4
Figure 3.....	7
Figure 4.....	8
Figure 5.....	9
Figure 6.....	12
Figure 7.....	13
Figure 8.....	15
Figure 9.....	17
Figure 10.....	18
Figure 11.....	21
Figure 12.....	22
Figure 13.....	24
Figure 14.....	26
Figure 15.....	28
Figure 16.....	31
Figure 17.....	33
Figure 18.....	34

Abstract

MASTER'S PROGRAM IN EARTH SYSTEM SCIENCE

Matthew Smith, M.S.

George Mason University, 2019

Thesis Director: Dr. Linda A. Hinnov

The Paleocene Eocene Thermal Maximum (PETM), also known as Eocene Thermal Maximum 1 (ETM-1) is a global warming spike that occurs within a long term warming trend in the early Cenozoic Era (56 million years ago). This spike has been detected in the paleoclimate record as a sudden global temperature increase of approximately 5°C and an associated increase in the amount of ¹³C-depleted carbon in the ocean. The Wilson Lake core from New Jersey, USA recorded the PETM event. The nearby Woodland Beach core drilled in Delaware, does not immediately appear to have recorded the PETM event. Whether or not the PETM is recorded within the Woodland Beach core is investigated in this thesis using available micro- and nanofossil information, planktonic and benthonic foraminifera, and sediment color intensity analysis. A possible record of the Eocene Layer of Mysterious Origin (ELMO), also known as the Eocene Thermal Maximum 2 (ETM-2) is also investigated. Data from benthonic and planktonic foraminifera counts and preservation, calcareous nanofossils, and sediment

color intensity collectively indicate that the most likely position of the Paleocene-Eocene boundary and start of the PETM is at a core depth of 407.8 ft.

1. Introduction

The Paleocene-Eocene Thermal Maximum (PETM) occurred approximately 56 million years ago (Ma) and lasted for about 200,000 years (McInerney and Wing, 2011). During this time, the average temperature of the global ocean increased by about 5°C, hypothesized to be due to a massive methane release to the atmosphere causing global warming. This is characterized by a strong excursion in both marine carbon and oxygen isotopes (**Figure 1**).

Evidence for the PETM includes a carbon isotope excursion (CIE) showing a rise in depleted ^{18}O , interpreted as an ocean temperature increase of approximately 5°C and a dramatic rise in ^{13}C -depleted carbon into the ocean (**Figure 1**) (e.g., Zachos et al., 2010). Carbon dioxide had a large impact on climate change throughout the Cenozoic Era with temperature changes including both long term warming and cooling. From 60 to 50 Ma (which includes the PETM) atmospheric CO_2 increased, largely from India subducting carbonate-rich ocean crust prior to colliding with Asia (Hansen et al., 2013). Within these long-term trends were global warming spikes, including the remarkably prominent PETM, which is thought to be the result of a massive methane hydrate release from destabilization of marine margin sediments, and lasted approximately 200 kyr (McInerney and Wing, 2011). The added carbon in the oceans would also have increased seawater acidity, potentially impacting the preservation of foraminifera and other oceanic calcifiers.

The Eocene Layer of Mysterious Origin (ELMO) is the second hyperthermal event of the Eocene that occurred at 54 Ma. Similar to the PETM it was a prominent transient warming event that occurred 1.83 myr after the PETM and lasted approximately 42 kyr. Both the PETM and ELMO have revealed cyclicity related precession and eccentricity that was used to establish age records (Westerhold et al., 2018).

Identifying the PETM and ELMO events in the Woodland Beach core, Delaware, USA, a major goal of this thesis, will enable calculation of an average sedimentation rate between the two events and the development of a chronology for the subsurface Mid-Atlantic Coastal Plain Paleocene-Eocene sequence in Delaware.

This thesis investigates the recently collected Woodland Beach core from subsurface Delaware, USA. The Woodland Beach core location is approximately 35 miles southwest from the well-known Wilson Lake core in New Jersey. The Wilson Lake core has had isotopic, foraminifera assemblage, lithologic, and gamma data collected and studied for PETM (Zachos et al., 2006). Another nearby core is the Bass River core, part of the Ocean Drilling Program, that had isotopic data collected to locate the onset of the PETM CIE as shown in **Figure 2** (Miller et al., 2003).

The proximity of the two cores makes them potentially ideal to use for comparisons. The core was scanned for color variations and, across the Paleocene-Eocene boundary interval, sampled for benthonic and planktonic foraminifera. The goal is to analyze foraminiferal patterns and core sediment color stratigraphic series to infer the location of the Paleocene-Eocene boundary interval in a nearshore shallow marine environment.

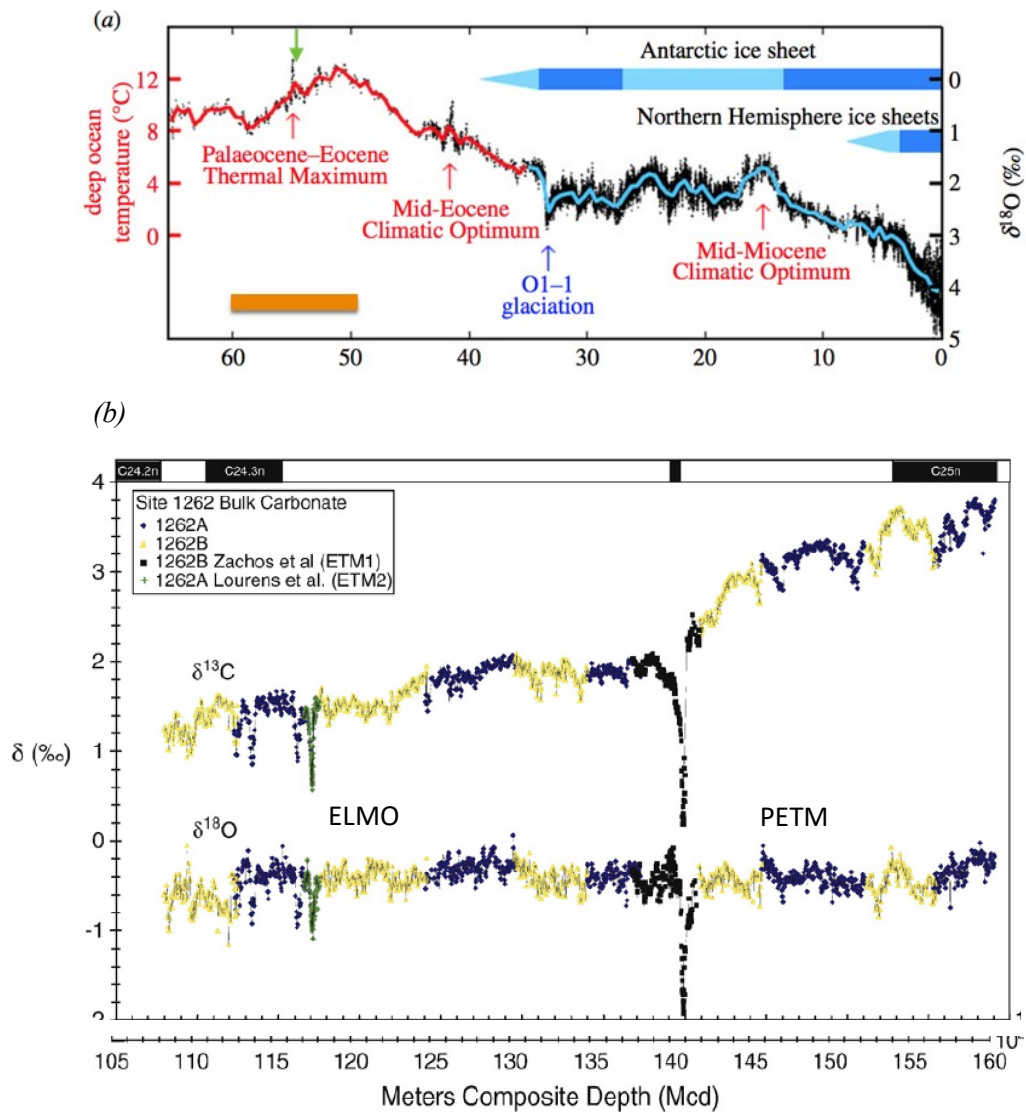


Figure 1: The evolution of deep ocean temperatures through the Cenozoic Era and early Eocene hyperthermals. a. Greatly depleted ^{18}O indicating the PETM occurs at the Paleocene-Eocene boundary (green arrow) based on the global record of benthonic foraminifera. (Modified from Hansen et al., 2013). The orange horizontal bar indicates the target portion of the Woodland Beach core, Delaware, USA that is investigated in this thesis. Up is to the right. b. Early Eocene hyperthermals, highlighted by significant spikes in bulk sediment $\delta^{18}\text{O}$ and $\delta^{13}\text{C}$ from Site 1262 (Walvis Ridge, South Atlantic) indicating sudden warming and carbon cycle perturbations related to a 200-kyr-long PETM (earliest Ypresian, 55.93 Ma to 55.73 Ma) and a 42-kyr-long ELMO (54.10 Ma to 54.058 Ma) (Westerhold et al., 2018). (Graphic modified from Zachos et al., 2010). Magnetochrons are shown at the top; up is to the left.

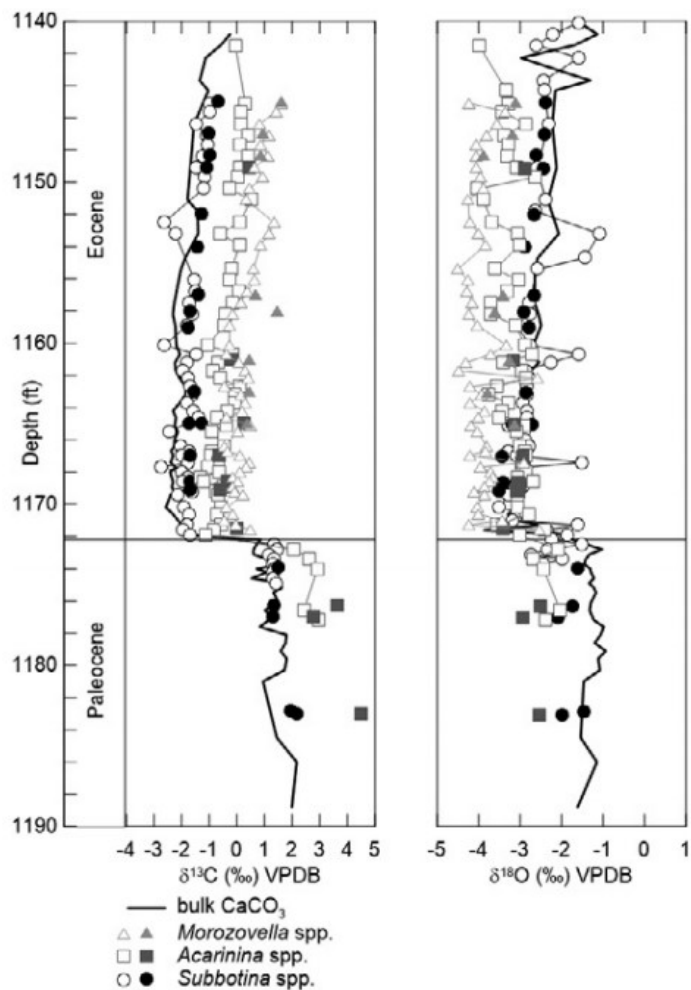


Figure 2: Start of the PETM CIE at 1178 ft in the Bass River core, New Jersey, showing $\delta^{13}\text{C}$ (left) and $\delta^{18}\text{O}$ (right) depletion from planktonic (*Acarina* and *Morozovella*) and benthonic (*Subbotina*) foraminifera (Babila et al., 2016). Systematic shifts between planktonic and benthonic values are due to ^{18}O and ^{13}C gradients in the water column from sea surface to seafloor. For location, see **Figure 4**.

What is interesting about the Woodland Beach core is that it does not appear to record the PETM in its entirety, in that it is apparently missing the definitive lithology of the Marlboro Clay (discussed further below), compared to similarly situated cores from New Jersey, notably the Wilson Lake core (Sluijs et al., 2006; Zachos et al., 2006).

The geological setting of the Woodland Beach core in the Mid-Atlantic Coastal Plain experienced multiple marine transgressions and regressions throughout the Cenozoic Era (Ward and Powers, 2004). Foraminifera ratios of planktonic versus benthonic counts provide information on these sea level variations. The sand percentage calculated from core samples indicate the evolution of depositional energy and sediment sources. The appearance of the calcareous nannofossil *D. araneus* allows for a positive identification of the PETM interval in the core. The Woodland Beach core is longer than other cores recently drilled in the region, and is expected to provide an expanded section of the PETM to ELMO interval. Stable isotopes were not obtained due to lack of funds. Red color intensity was used to infer isotope data as a cheaper (“free”) method. Isotope data will be completed in the future for identification of the CIEs related to the PETM and ELMO, and will be compared to the red intensity series.

2. Data

2.1 Geological setting

The arches and embayments of the Mid-Atlantic Coastal Plain are the result of tectonics and faulting related to the widening of the Atlantic Ocean (Ward and Powers, 2004) (**Figure 3**). The location of the Woodland Beach core is in the Salisbury Embayment, in northern Delaware. The Salisbury Embayment experienced multiple marine transgressions and regressions throughout the Mesozoic and Cenozoic eras, during which depositional environments alternated from fluvial, deltaic to shallow marine shelf and back again. Significant portions of the embayments remained in marine conditions through much of this time, including the Woodland Beach core location.

Reconstructions of the paleodepths of the New Jersey cores indicate paleodepths of 40 m (pre-PETM) to 60 m (PETM) at Wilson Lake, 80 m (pre-PETM) to 100 m (PETM) at Bass River, and 60 m (pre-PETM) to 80 m (PETM) at Millville, according to Makarova et al. (2016) (their Fig. 7). Assuming that bathymetry roughly parallels the coastline that characterized the Mid-Atlantic during PETM time, Woodland Beach would correspond to the Millville location, Makarova et al. (2016) (their Fig. 1), i.e., have a pre-PETM depth of 60 m and a PETM depth of 80 m.

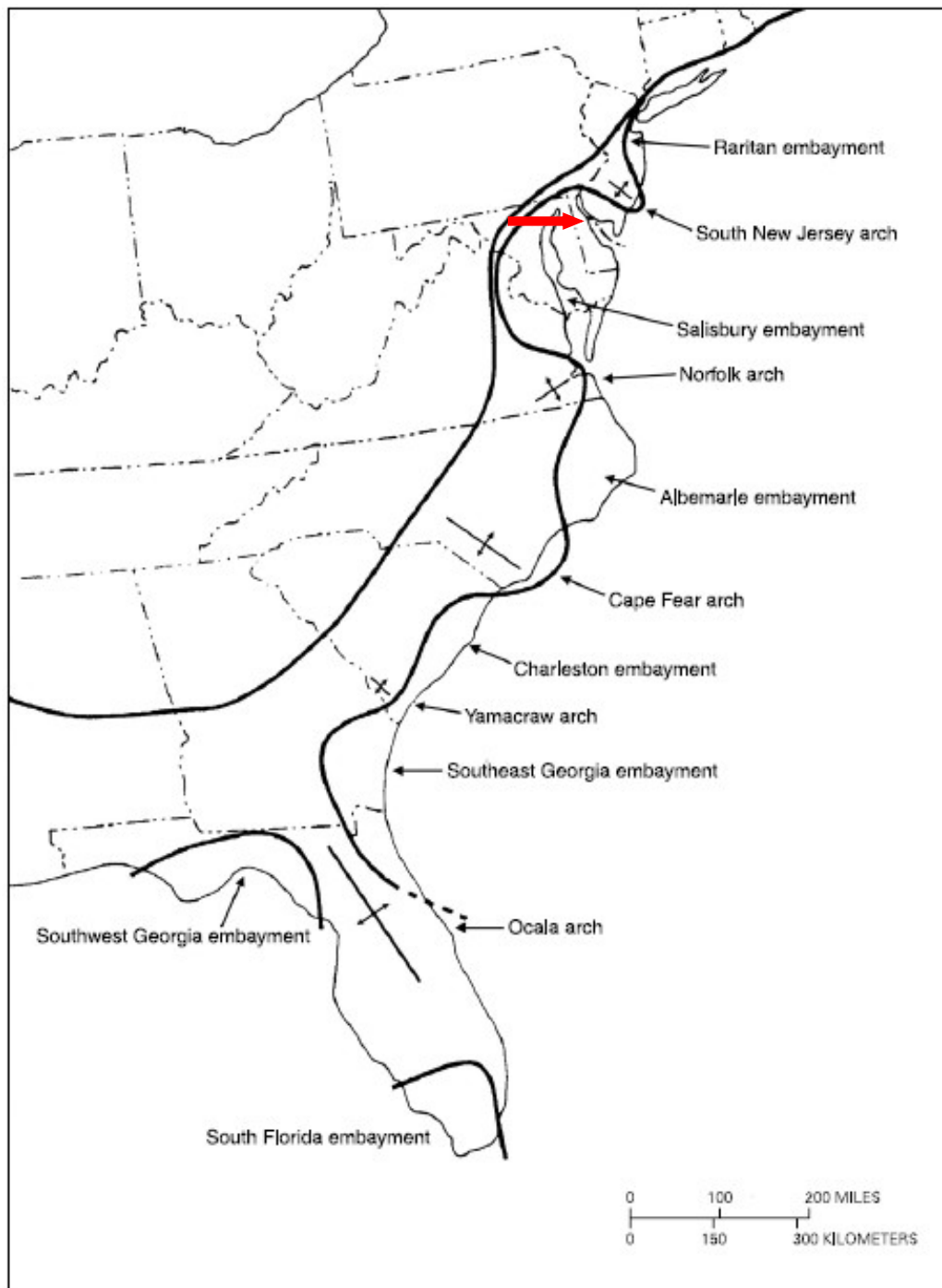


Figure 3: Map of the US Atlantic Coastal Plain (from Ward and Powers, 2004). The Woodland Beach core is in the Salisbury Embayment in northern Delaware (red arrow). The seaward black lines delineate the arches and embayments; the landward black line shows the westward limit of marine deposition.

2.2 The Woodland Beach core

The 820.2 ft long Woodland Beach core in Delaware, USA was drilled by the United States Geological Survey from May 2 to May 12, 2012 (**Figure 4**). Photographs of the core, standard well logs, and drilling notes are available in addition to the core itself. 75 sections of the core were drilled and documented. These were split into 2 ft sections and 113 photographs were taken of the core sections. The core is stored in the core repository of the Delaware Geological Survey, in Newark, Delaware. **Figure 5** compares the Woodland Beach and Wilson Lake cores, showing a comparable thickness of the two cores, but notably, there is an absence of the “Marlboro” clays in the Woodland Beach core due to either faulting, or the terrestrial clays bypassed the Woodland Beach core location, for example, if it was on a local high.

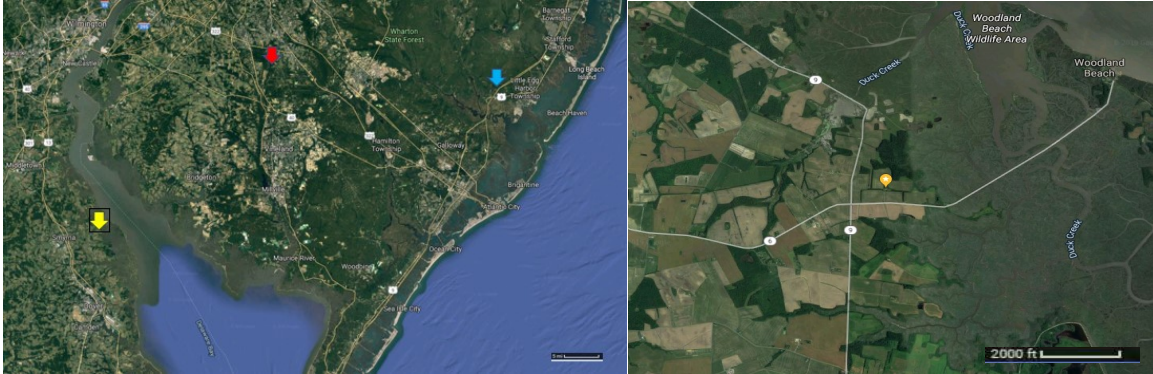


Figure 4: Left image shows the location of the Woodland Beach core in Delaware, the yellow tag, at GPS coordinates 39.313582° North and $75.50951610873977^{\circ}$ West, the Wilson Lake core in New Jersey, the red tag, at GPS coordinates 39.659833° North and 75.047167° West, and the Bass River core, the blue tag, at GPS coordinates 39.611700° North and 74.436700° West (Miller et al., 2003). The right image zooms in on the Woodland Beach core location. (Images taken from Google Maps)

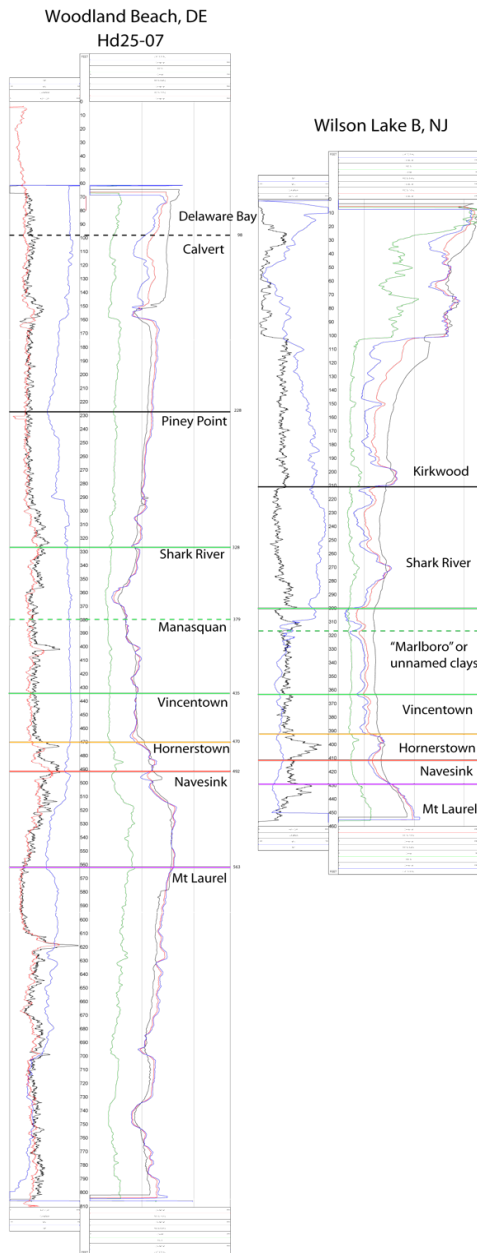


Figure 5: Comparison of the well logs of Woodland Beach core, Delaware and Wilson Lake core, New Jersey. “Marlboro” clay is missing from the Woodland Beach core (above the Vincentown Formation). Logs include gamma ray (black), spontaneous potential (blue), short normal resistivity (red), point resistance (green), long normal resistivity (black), and lateral resistivity (blue). The indicated formations are inferred from drilling notes.

2.3 Well logs

The Woodland Beach core gamma ray and spontaneous potential well logs are shown in **Figure 6**. Gamma ray data were used as preliminary markers to delineate by DGS, by comparing the gamma ray patterns with previously studied cores, e.g., the Wilson Lake core. Gamma ray spectrometers measure the natural radiation of sediment, elevated for organic matter or clay, or in the Woodland Beach core, glauconite. The base of the PETM is expected to be near a depth of 400 ft, i.e., at the Paleocene-Eocene boundary, just above the Vincentown-Manasquan formation boundary. Numerous other cores in the New Jersey-Delaware-Maryland tristate area contain the kaolinite-rich Marlboro Clay (Harris et al., 2010; Self-Trail et al., 2017), which has been found to co-occur with the CIE of the PETM. The absence of the Marlboro Clay in the Woodland Beach core may signal that an unconformity occurs around 400 feet, and that the PETM has not been recorded.

The logs track sediment changes from high sand content and large amounts of glauconite at positions with high gamma ray values. Sand is the size of sediment grains between 63 μ m and 2 mm. It takes greater energy to move larger grain sizes, thus more sand equates to higher energy environments. (These larger grains will also drop out first when energy drops.) There are exceptions, such as in this case, sand-sized glauconite grains which grow in situ on seafloor experiencing no deposition. Glauconite is a clay mineral that forms within low oxygen marine environments, most commonly between depths of 30 to 700 meters among decaying organic matter (Porrenga 1967). The drilling notes indicate that the core sediment is comprised of sands, silts and clays, glauconitic intervals, shelly or calcareous intervals, and phosphate nodules (near the PETM), and

sediment colors ranging from light to dark brown, light to dark gray, light to dark green-gray, olive-gray, red, orange, and yellow. Changes in sediment color indicate lithological changes, e.g., sand rich in organic matter is darker and greener than sand without organic matter, which tends to be more red. Sediments that are red may be oxidized, indicating higher oxygen levels affecting mineralogy. A change in color can also indicate a change in the sediment source, or faulting within a core, resulting in loss of recorded time.

The PETM is expected to occur in the lower Manasquan Formation at a depth between 401-414 ft (**Figure 6**). A major goal of this thesis is to determine the position of the Paleocene-Eocene boundary in the core, and to characterize the sedimentary record of the interval that most likely recorded the interval including the PETM and ELMO hyperthermals.

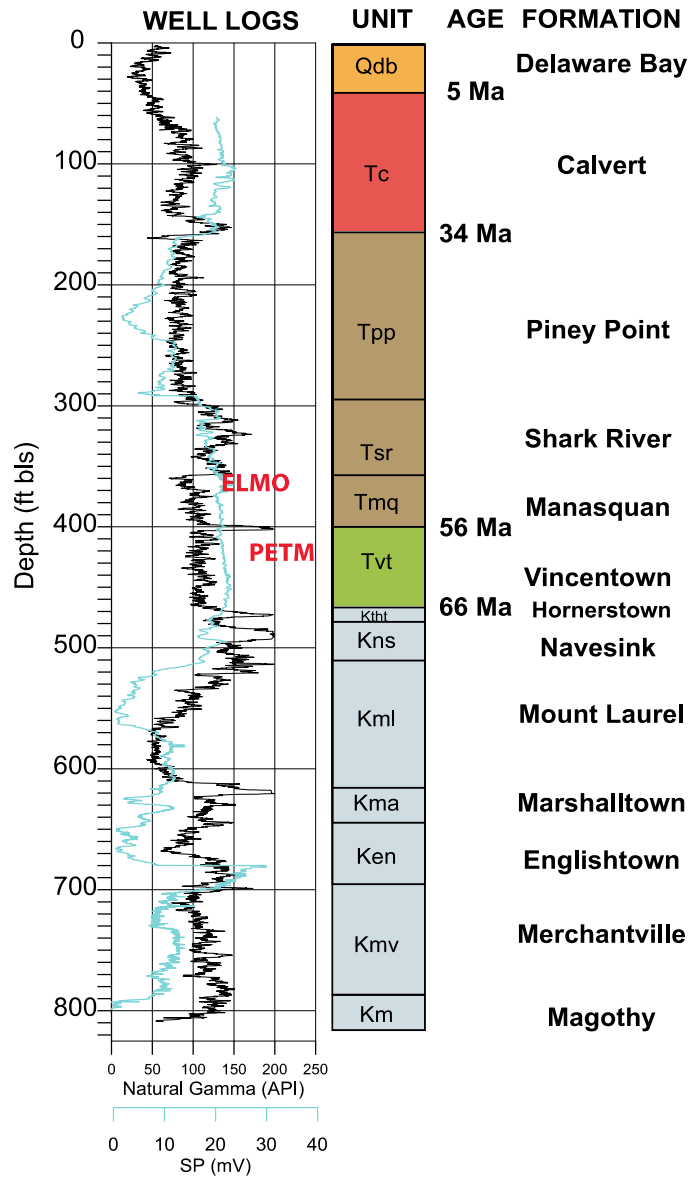


Figure 6: Gamma and spontaneous potential of the Woodland Beach core on the left, provided by the Delaware Geologic Survey. The right shows a stratigraphic column with formations and key boundary ages from Vandenberghe et al. (2012). The core is missing a number of Miocene-aged formations that have been identified elsewhere in the Mid-Atlantic Coastal Plain (i.e., the Choptank, St. Mary's, Cat Hill and Bethany formations). Important revisions to the location of the Manasquan and Vincentown formation boundary is discussed below in **Section 5.1**. Inferred stratigraphic positions of the PETM and ELMO hyperthermals are shown in red text.

2.4 Foraminifera and Calcareous Nannofossils

Foraminifera were picked from 29 samples along the core, from the likely PETM to ELMO stratigraphic interval. The foraminifera were counted in order to study patterns in the relative number of benthonic and planktonic foraminifera at each core depth, along with their preservation. At least three taxa are expected: the planktonic foraminifera *Morozovella velascoensis* and *Acarinina soldadoensis* and the benthonic foraminifer *Cibicidoides* sp. (**Figure 7**), but the entire assemblage has not yet been established for Woodland Beach. Varying ratios of planktonic to benthonic counts in the samples may indicate paleo-environmental changes, e.g., sea level fluctuations. Since global sea level was moderately to very high during the Paleocene and Eocene epochs (Miller et al., 2014) generally high numbers of planktonic foraminifera in the samples are expected.

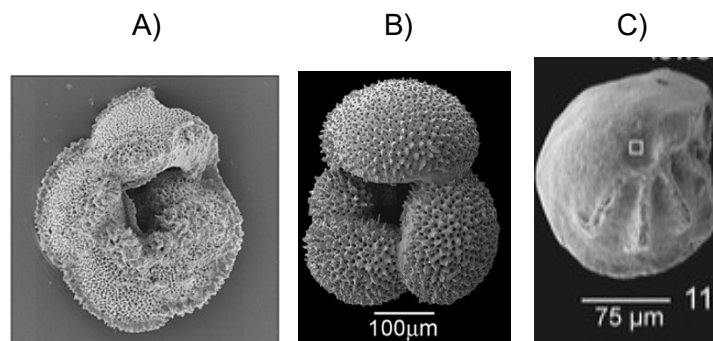


Figure 7: Electron microscope images of three foraminifer genera used in Zachos et al. (2006) for stable isotope analysis. A) *M. velascoensis* (Zachos et al., 2006), B) *A. soldadoensis* (http://www.mikrotax.org/pforams/index.php?dir=pf_cenozoic/muricate%20non-spinose/Truncorotaloididae/Acarinina/Acarinina%20soldadoensis); and C) *Cibicidoides* sp. (Stassen et al., 2012).

In addition to the foraminifera, Dr. Jean Self-Trail (USGS) identified the calcareous nannofossil *Discoaster araneous* in the 401.1 ft sample but not in the 414.1 ft sample. This indicates that the base of the PETM is between 401.1 and 414.1 feet (details in **Section 5.1**).

2.5 RGB intensity scans of core photographs

Color intensity scans are increasingly used to characterize drill core photographs (Francus, 2007; Nederbragt and Thurow, 2007). The goal of measuring a Red-Green-Blue (RGB) intensity series through the entire Woodland Beach core is to provide a high-resolution proxy for lithology that can be used to search for Milankovitch cycles and potential hiatuses. The relative intensities of these three primary colors combine to produce all other colors. Blue is not well understood as a sediment color, while red and green are used as a crude proxy for oxidized (red) vs. reduced (green) sediment.

The Woodland Beach core photographs were scanned using ImageJ (NIH freeware; <https://imagej.nih.gov/nih-image/>); a transect along the center of each core section was analyzed for RGB color intensity (**Figure 8**). The relative intensities of these three primary colors can be combined to produce all colors along the core. Red color intensity is used here as an indicator of oxygen level at time of deposition: high red intensity indicates oxidized sediment and low intensity indicates anoxic sediment.

The scans of the individual core sections were then spliced together to show the full core, with missing sections labeled as 99999 to represent the blank, for a total of 1,162,210 pixels. This composite intensity series was then exported into MATLAB and using *depthtotime.m* the pixel scale was converted from pixel scale into core depth in

feet (totaling 820). Time series analysis was conducted on the R series (**Sections 4.3 and 5.3**).

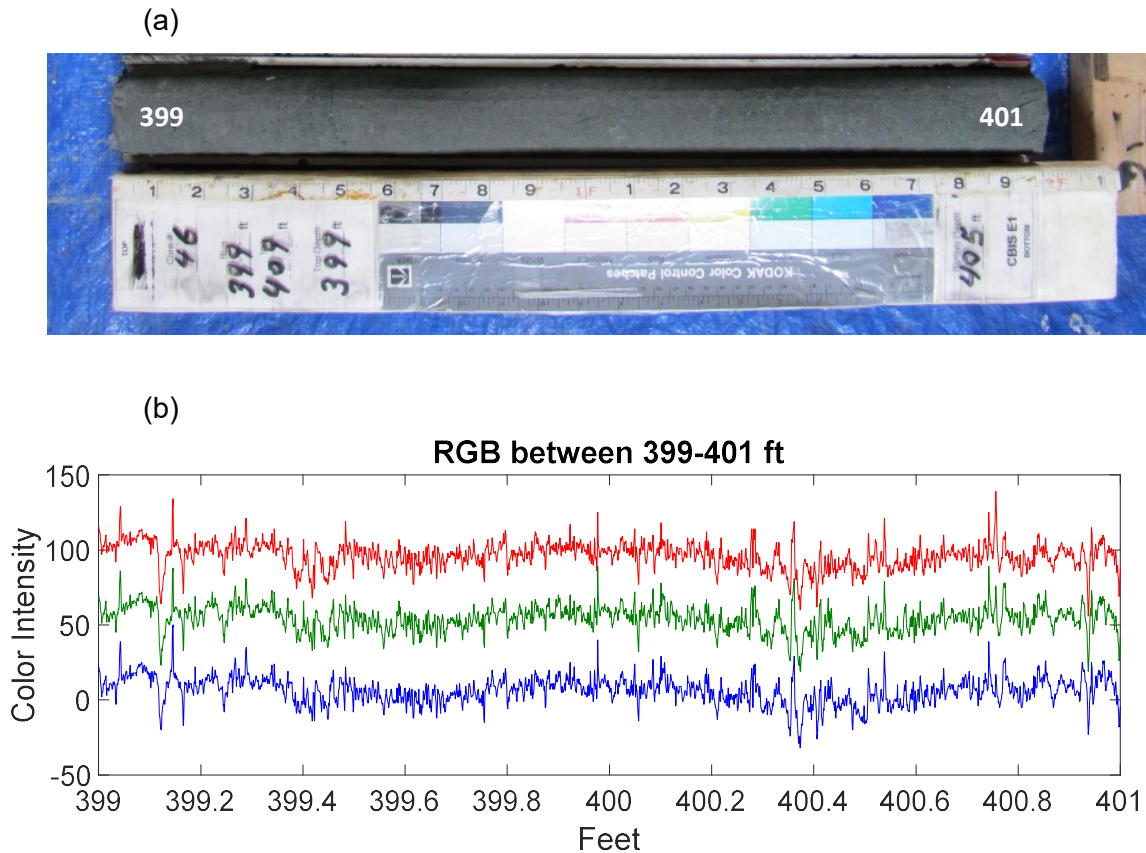


Figure 8: (a) Photograph of the Woodland Beach core sections 399-401 ft. (b) Red (top), green (middle), and blue (bottom) intensities between 399-401 ft. To show them separately 50 intensity values were subtracted from green, and 100 intensity values from blue. The intensities closely resemble each other, but have relative differences that, when combined, recreate the color of the core as a function of core depth.

The red intensity series provides a crude indication of oxygen levels at the depositional site, i.e., low red intensity may indicate reducing conditions, and high red intensity oxidizing conditions. This would be useful in identifying the PETM, which is associated with high sea level, global warming, increased productivity, and potentially

lower oxygen levels in shelf paleo-environments such as those represented at Woodland Beach.

3. Methods

3.1 Core sampling

29 samples were collected from the Woodland Beach core at the core repository in the Delaware Geological Survey in Summer, 2017 (**Table 1**). A 1/10 foot of sample was sliced from the core every two feet, from 357 to 414 feet (**Figure 9**).



Figure 9: Two samples taken from the Woodland Beach core. A 1/10 ft sample was taken every 2 ft.

3.2 Sample preparation for foraminifera

Half of the samples were reserved for future organic carbon isotope analysis and other geochemistry. At the USGS, samples were cleaned in Dr. Marci Robinson's lab using phosphate-rich Calgon and ultra-pure water and sieved with a stainless steel >63 μm sieve. Samples were then split into similar amounts to estimate comparable foraminifera concentrations. All identifiable *Cibicidoides*, *Morozovella*, and *Arcarinina* foraminifera were picked and stored on microscope single cell microfossil slides. **Figure 10** shows examples of planktonic and benthonic foraminifera in three Woodland Beach samples.

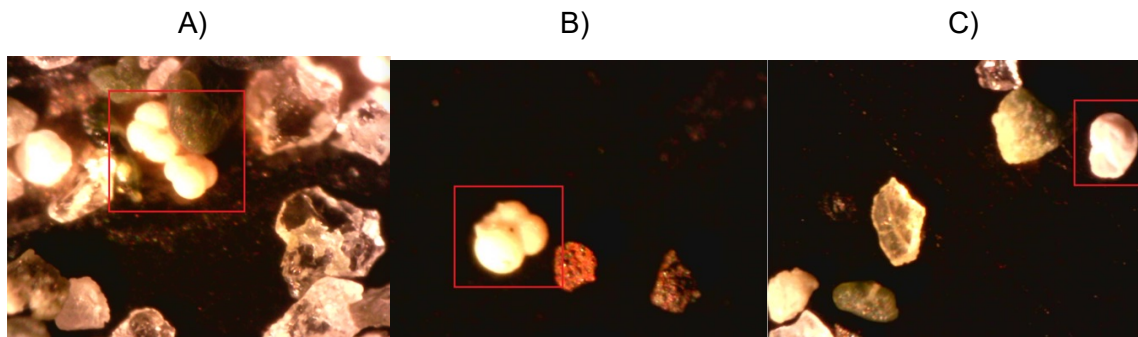


Figure 10: Microphotographs of Woodland Beach core samples that contained foraminifera indicated by the red boxes. A) WBMS3 (361.0-361.1') with planktonic foraminifera. B) WBMS5 (365.0-365.1') with a planktonic foraminifer. C) WBMS11 (377.0-377.1') with a benthonic foraminifer.

3.3 Time series methods

Time series analysis was conducted on the red intensity series, with the goal of evaluating possible Milankovitch cycles.

- (1) Pixel to depth conversion was accomplished by assigning the top of the red intensity series to a core depth of 0 ft, and the base of the series to a core depth of 822 ft, and assigning each of the 1162210 pixel values to increments of 822 ft / 1162210, from top to bottom.
- (2) LOESS (“Locally Estimated Scatterplot Smoother”) curve estimation involving 2nd order polynomial fitting of a running window was done with *smooth.m* provided in MATLAB’s Curve Fitting Toolbox, to estimate and remove strong lighting artifacts (see **Section 4.4**) resulting in a “residual red intensity series.”
- (3) Power spectral analysis of the residual red intensity series was done with the multitaper estimator *pmtm.m* provided in MATLAB’s Signal Toolbox.
- (4) A FFT (Fast Fourier Transform) spectrogram was computed to evaluate the persistence and distribution of spectral power throughout the residual red intensity series using the MATLAB script *evofft.m* provided at:
<http://mason.gmu.edu/~lhinno/cyclostratigraphytools.html>
- (5) Bandpass filtering was carried out on the frequency band of the residual red intensity series most likely to contain precession cycles

using *tanerfilter.m*, available at:

<http://mason.gmu.edu/~lhinnov/cyclostratigraphytools.html>

(6) Hilbert transformation was applied to evaluate amplitude envelope of the bandpass filtered series, using *hilbertsignal.m*, available at:

(7) <http://mason.gmu.edu/~lhinnov/cyclostratigraphytools.html>

(8) The La2004 astronomical solution of Laskar et al. (2004) was downloaded from:

<http://vo.imcce.fr/insola/earth/online/earth/La2004/index.html>

The La2004 astronomical solution is a detailed model of Solar System planetary motions that dictate the Earth's orbital eccentricity, obliquity and precession variations. It is reported in 1 kyr intervals back through time. The precession index and orbital eccentricity variables of the solution for the PETM to ELMO time interval, from 56.5 to 54 Ma, will be compared with the Woodland Beach core red intensity series (see **Section 5.3**). Different astronomical solutions agree back to 50 Ma, but then diverge prior to 50 Ma, depending on initial conditions (Laskar et al., 2004). The PETM to ELMO interval occurs just prior to 50 Ma, and so there is no guarantee that the La2004 solution adopted for this thesis is the most accurate solution.

3.4 Artifacts: estimation and removal

Strong and pervasive 1 to 2 ft cycles were observed along the R and G series and identified as artifacts created by uneven camera lighting along the 2 ft sections of core (example in photo shown in **Figure 8**). To remove these artifacts, MATLAB's *smooth.m* was applied with the LOESS algorithm and a 1500 pixel-long window, to calculate a smoothed curve for each core section that was then subtracted from the intensity series (**Figure 11**). This process was repeated for each core section from 350-420 ft, for the R and G intensity series separately. The results for the R intensity series is shown in **Figure 12**.

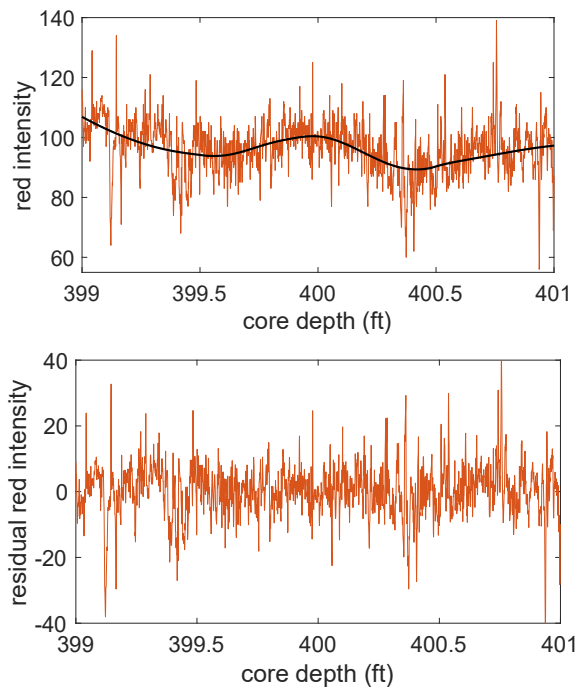


Figure 11: Top: The raw red intensity series (red) and smoothed LOESS curve (black) estimating the lighting artifact affecting the 399-401 ft core section. Bottom: The residual red intensity series after the smooth curve has been subtracted.

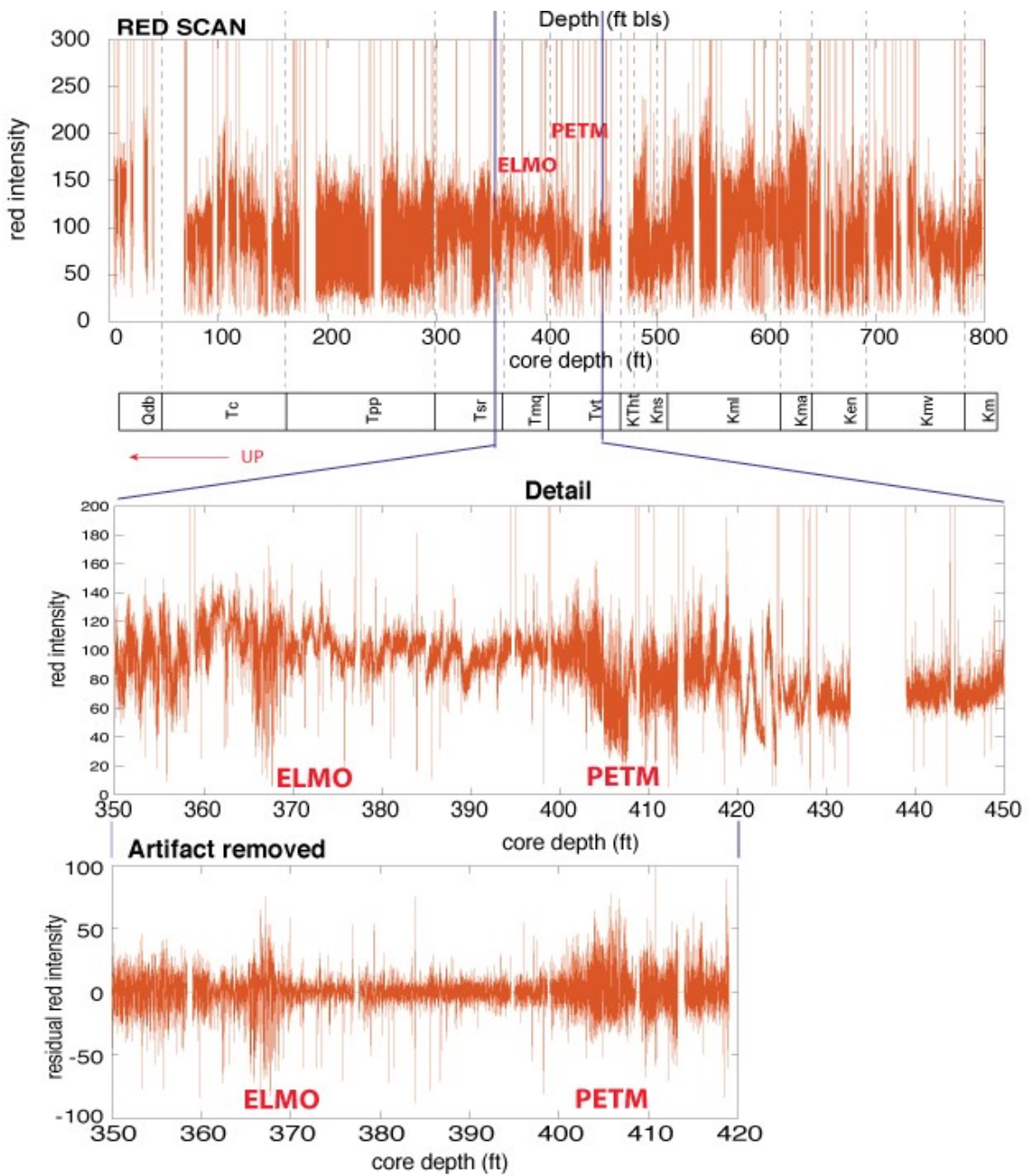


Figure 12: Woodland Beach core red intensity and residual red intensity series. From top to bottom: (a) raw red intensity scan of entire core, (b) formations (see **Figure 6** for definition of abbreviations), (c) detail between 350-450 ft, highlighting strong 2 ft cycle artifacts, and (d) section between 350-420 ft after removal of artifacts.

4. Results

4.1 Benthonic and planktonic foraminifera count

The number of planktonic and benthonic foraminifera recovered from 357 ft to 414 ft in the Woodland Beach core are listed in **Table 1** and plotted in **Figure 14**. The bulk counts of foraminifera reveal lower count of planktonic than benthonic from WBMS29 (414 ft) through WBMS27 (411 ft). WBMS26 (407 ft) has only 2 planktonic foraminifera and no benthonic foraminifera. There is a higher count of planktonic than benthonic from samples WBMS25 (405 ft) through WBMS22 (399 ft). At WBMS23 (401 ft) and again at WBMS21 (397 ft) there are an equal count of planktonic and benthonic foraminifera. WBMS20 (395 ft) has lower count of planktonic than benthonic foraminifera. WBMS19 (393 ft) through WBMS13 (381 ft) has higher count of planktonic than benthonic foraminifera. WBMS9 (371 ft) through WBMS4 (363 ft) have lower count of planktonic than benthonic foraminifera. WBMS3 (361 ft) through WBMS1 (360 ft) present a return to higher sea levels. WBMS4 (363 ft) shows a much higher count of benthonic foraminifera than the rest of samples.

4.2 Percent sand record

Sand percentage was calculated from vial weight post foraminifera processing divided by the dry weight preprocessing, values seen in **Table 1**. Sand percentage from 367 to 357 ft was not collected due to starting foraminifera cleaning before recording dry weight. The percentage of sand is at 63.5% at 414 ft within the core. This drops to 42.5% at 409 ft. 407 ft a dramatic increase in sand occurs, reaching 90.9%. The sand percentage then gradually decreases to 22.8% at 397 ft, before showing small fluctuations in increasing and decreasing sand percentage up to 18.7% at 375 ft. This is followed by a stark decrease to 3.8% at 373 ft and 0.7% at 369 ft. The dramatic increase in sand percentage occurs at 407 ft (**Figures 13, 14**).

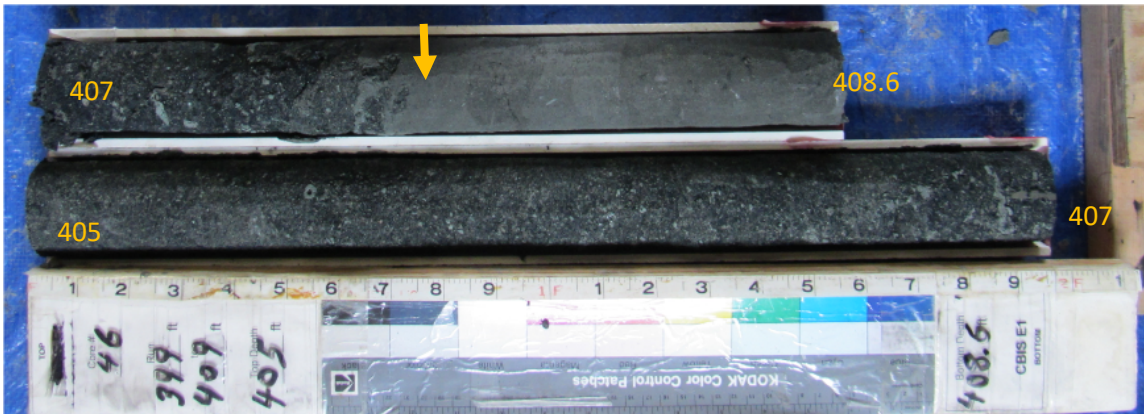


Figure 13: Photo of 405 ft to 408.6 ft core sections. At 407.7 ft (arrow) there is a dramatic increase in sand percentage toward the top of the core accompanied by an increase in glauconite (from drilling notes).

Table 1. Samples from the Woodland Beach core. Samples were taken every 2 feet and were 1/10 of a foot in length.

*Not taken from XXX.0-XXX.1 ft because of lack of adequate sediment.

^Taken at 414 ft instead of 413 ft due to missing section.

Sample	Sample Depth (ft)	Dry Wt. (g)	Vialed Wt. (g)	Splits	Planktonic	Benthonic
WBMS1	357.0-357.1	-	22.55	5	15	2
WBMS2	359.0-359.1	-	10.79	4	16	1
WBMS3	361.0-361.1	-	15.88	4	14	5
WBMS4	363.0-363.1	-	0.09	0	12	219
WBMS5	365.0-365.1	-	0.00	0	1	7
WBMS6	367.0-367.1	-	0.09	0	10	6
WBMS7	369.0-369.1	31.91	0.22	0	4	26
WBMS8	371.0-371.1	17.86	0.15	0	3	26
WBMS9	373.0-373.1	20.84	0.79	0	2	11
WBMS10	375.0-375.1	32.32	6.03	3	8	12
WBMS11	377.0-377.1	18.87	2.17	1	21	13
WBMS12	379.0-379.1	19.42	3.12	1	11	11
WBMS13	381.0-381.1	14.90	2.93	1	34	10
WBMS14	383.0-383.1	47.00	6.53	3	27	4
WBMS15	385.0-385.1	34.96	4.38	2	32	6
WBMS16	387.0-387.1	25.98	4.21	2	8	1
WBMS17	389.1-389.2*	23.07	6.49	3	11	4
WBMS18	391.0-391.1	35.64	10.54	4	16	3
WBMS19	393.0-393.1	40.53	12.11	4	15	3
WBMS20	395.1-395.2*	29.40	6.94	3	4	17
WBMS21	397.0-397.1	24.38	5.57	3	22	22
WBMS22	399.1-399.2*	17.97	5.90	3	11	6
WBMS23	401.0-401.1	17.31	6.22	3	17	16
WBMS24	403.0-403.1	24.02	12.64	4	9	3
WBMS25	405.0-405.1	30.95	23.17	5	29	10
WBMS26	407.1-407.2*	26.27	23.88	5	2	0
WBMS27	409.1-409.2*	34.31	14.57	4	7	10
WBMS28	411.0-411.1	25.04	12.65	4	5	7
WBMS29	414.0-414.1^	18.12	11.51	4	4	6

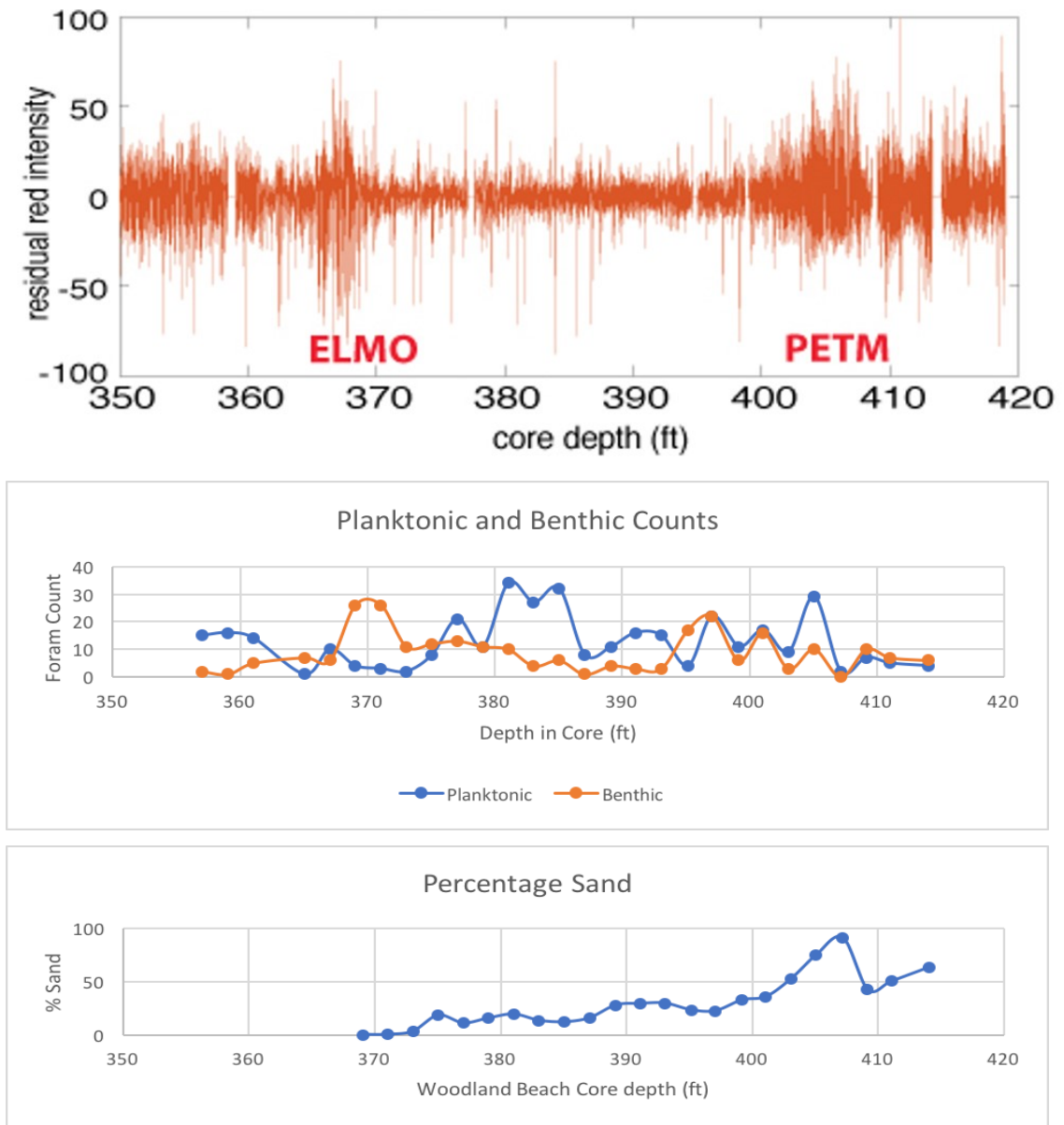


Figure 14: Top: The residual red intensity series from 350-420 ft. The ELMO is inferred at 368 ft and the PETM starting at 408 ft, a 40 ft separation representing 1.83 Myr (details in **Section 5.1, 5.3**). Middle: Counts of benthonic and planktonic foraminifera recovered from 350 to 414 ft in the Woodland Beach core (values listed in **Table 1**). Bottom: Percent sand estimated from processing foraminifera. Note: sample WBMS4 not plotted due to an extremely high outlier benthonic count, so the fluctuations can be better visualized.

4.3 Spectral analysis of the residual red intensity series

Spectral analysis reveals that the residual red intensity series has a very “noisy” power spectrum with multiple spectral peaks (**Figure 15**). This noisiness reflects a high degree of randomness in the sediment deposition at Woodland Beach, with highly variable sedimentation rates and sediment facies changes. The power spectrum assesses the proportion of the variance of a time series as a function of frequency.

Power occurs preferentially in the frequency band from $f=2$ cycles/ft to 4 cycles/ft through most of the series, as indicated in the FFT spectrogram. This indicates a high incidence and persistence of 0.5 ft to 0.25 ft cycles throughout the residual red series. There is also high power at higher frequencies (see arrows), which originates from a limited part of the residual red series that has high amplitude variability, from 360 ft to 370 ft (inferred ELMO interval). Possibly sedimentation rates here are much lower, or sediments are unusually compacted in this interval. The FFT spectrogram also reveals evidence for multiple hiatuses, shown by “ringing” of power across all frequencies at approximately 6 ft intervals along the series (white triangles).

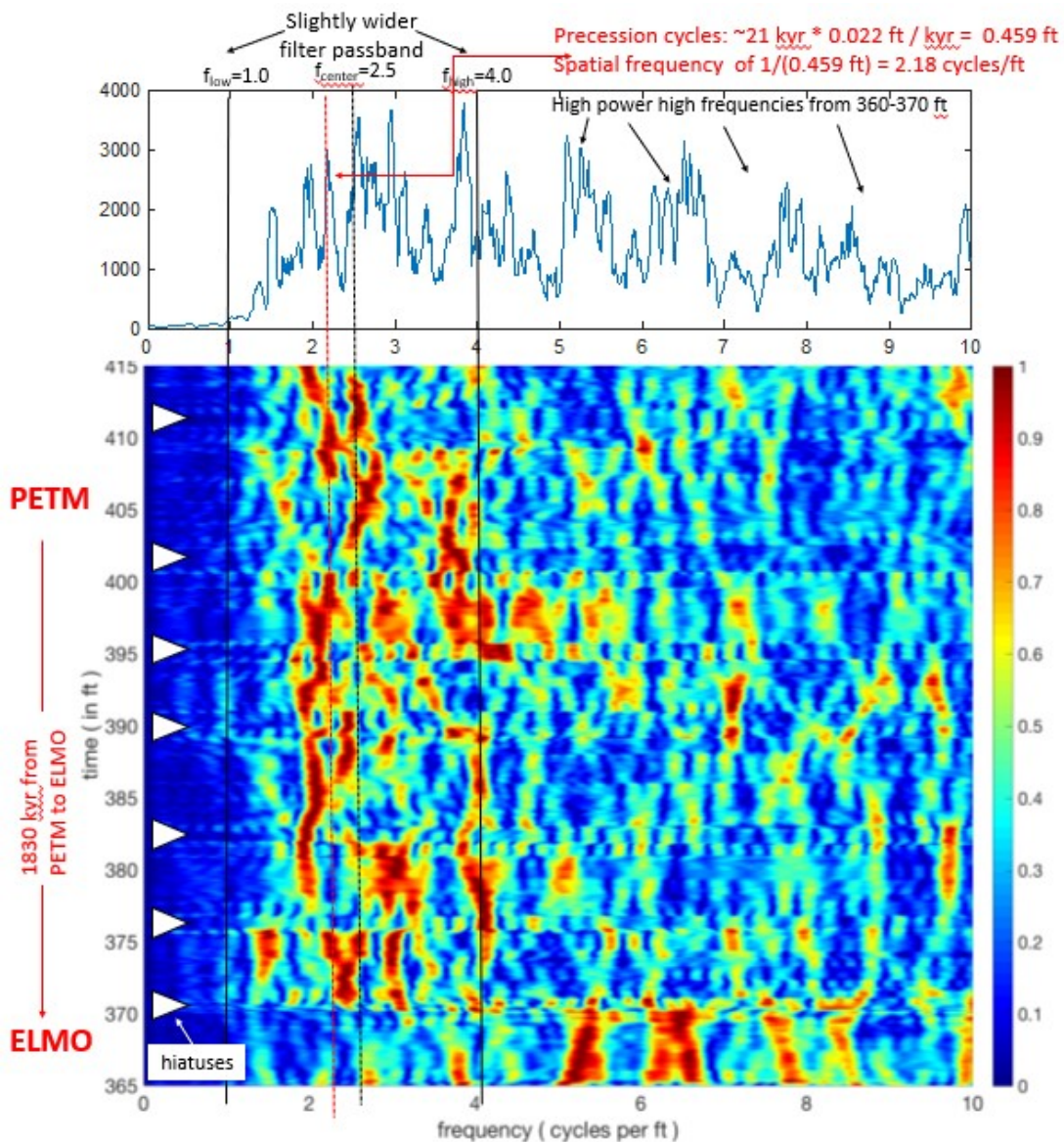


Figure 15: Spectral analysis of 350 ft to 420 ft. Top: 4π multitaper power spectrum of the entire interval. Bottom: FFT spectrogram between 365-415 ft. The running window is 5 ft. Hiatuses appear about every 6 ft. There is an occurrence of high power in the 2-4 cycles/ft band. Power in the 0-1 cycle/ft band are suppressed as a result of removing the 2 ft core photograph artifacts. White triangles indicate potential hiatuses. The black vertical lines indicate the passband of the bandpass Taner filter applied to isolate possible precession index cycles. Red annotations are discussed in **Section 5.3**.

5. Discussion

5.1 A preliminary biostratigraphy for the Woodland Beach core

Dr. Jean Self-Trail of the USGS has found that the sample at 404.1 ft is in calcareous nannoplankton NP10 Zone, before the carbon isotope excursion (CIE) in the Manasquan Formation. The sample at 414.1 ft has the nannofossil *Discoaster araneus*, placing it within the NP9a or NP9b Zone (Bralower and Self-Trail, 2016; Bukry, 1971) (**Figure 16**). The benthonic and planktonic foraminifera at 414 ft are of Eocene age (Robinson, 2019 personal communication). This suggests that 414 ft is NP9b and the base of the PETM is just below it.

To pinpoint the base of the PETM, foraminifera counts and the CIE's of other confirmed PETM cores can be compared. The PETM is associated with the largest benthonic foraminifera extinction in the last 90 Ma, resulting in 30-50% depletion of benthonic foraminifera diversity (McInerney and Wing, 2011). In the Woodland Beach core, where the inferred PETM begins (around 407 ft core depth), a decrease in benthonic foraminifera diversity should be observed. In fact, there were zero benthonic foraminifera recovered at the 407 ft level (sample WBMS26, see **Table 1**). Also during the PETM, planktonic foraminiferal geographic ranges shifted due to the increased temperatures (p. 501, McInerney and Wing, 2011). For example, the tropical genus *Morozovella* shifted to higher latitudes, including at Wilson Lake (notably, northward from the Woodland Beach core) during the early stages of the PETM.

5.2 Evidence for variable sea levels in the early Eocene

The planktonic and benthonic foraminifera recovered from 357 ft to 414 ft in the Woodland Beach core (**Table 1**) may indicate sea level oscillations. The bulk counts of foraminifera reveal higher numbers of benthonic to planktonic foraminifera from WBMS29 through WBMS27, indicating relatively low sea level. WBMS26 has only 2 planktonic foraminifera and no benthonic foraminifera. Planktonic outnumber benthonic foraminifera from samples WBMS25 through WBMS22, indicating relatively high sea level. At WBMS23 and again at WBMS21 there are an equal number of planktonic and benthonic foraminifera suggesting a lowering of sea levels. WBMS20 has more benthonic than planktonic foraminifera confirming a shift to low sea levels. WBMS19 through WBMS13 return to greater planktonic numbers indicating a shift back to higher sea levels. WBMS9 through WBMS4 show much higher numbers of benthonic, indicative of a lower sea level for a significant amount of time. WBMS3 through WBMS1 present a return to higher sea levels. WBMS4 shows an anomalously high number of benthonic foraminifera compared to the rest of samples. Sample WBMS26 at 407.1-407.2 ft shows the strongest evidence for the base of the PETM with lack of benthonic foraminifera and poor preservation possibly due to increased ocean acidification.

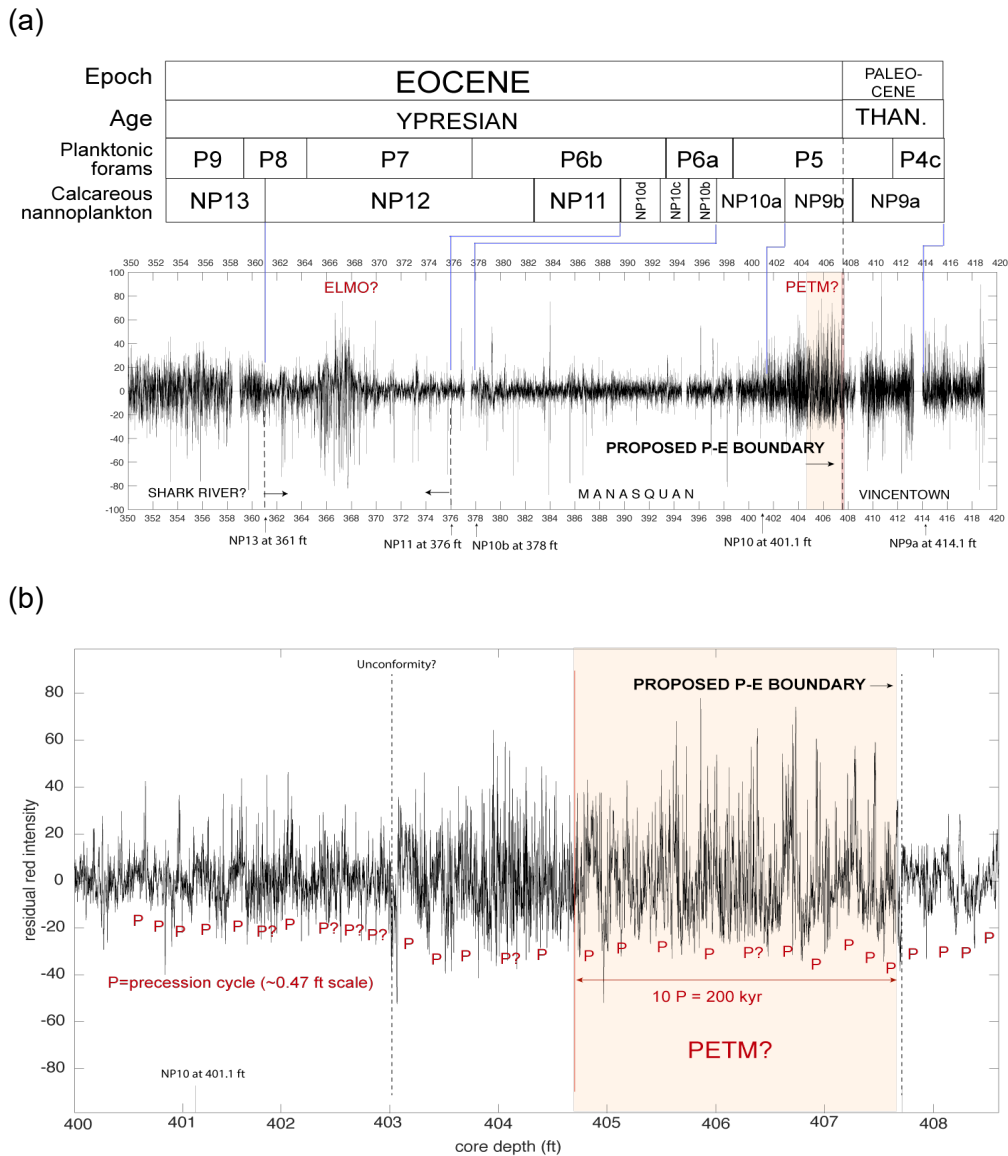


Figure 16: (A) The residual red intensity series with positions for calcareous nannofossils found by Dr. Jean Self-Trail (USGS, personal communication, 2018) (NP10 at 401.1 ft, NP9a at 414.1 ft) and M.-P. Aubry (Rutgers) communicated in 2019 by P. McLaughlin (DGS) (NP13 at 361 ft, NP11 at 376 ft, NP10b at 378 ft) and Lower Eocene global biostratigraphic zones for calcareous nannofossils and planktonic foraminifera (Arreguin-Rodriguez et al., 2018). The Manasquan Formation is early Eocene in age and represented by calcareous nannofossil Zones NP12, NP13, and lower NP14 (Owens et al., 1988). NP12 has not been identified, and so the Shark River/Manasquan boundary is somewhere between the two vertical dashed lines with arrows bracketing the ELMO. (B) Detailed residual red intensity series between 400-409 ft; the shaded zone is a proposal for the most likely PETM interval; interpreted precession cycles are marked with red “P”.

5.3 An Interpretation of Milankovitch cycles

The PETM and ELMO have been inferred at intervals of relatively low red intensity within the Manasquan Formation. The low red intensity could possibly indicate elevated reducing conditions in the sediment. The duration between PETM and ELMO has been estimated from deep sea cyclostratigraphy as 1830 kyr (Lourens et al., 2005; Westerhold et al., 2007). There is 40 ft between the inferred ELMO and PETM events (**Figure 16**), allowing an estimate of the average sedimentation rate for the interval: $40 \text{ ft} / 1830 \text{ kyr} = 0.021857 \text{ ft/kyr}$. Multiplying this by the average precession cycle period of 21 kyr indicates that 0.459 ft sedimentary cycles would be the most likely wavelength that has recorded precession cycles in the inferred PETM-ELMO interval. The inverse of 0.459 ft indicates a frequency of 2.18 cycles/ft (**Figure 15**).

The absence of power in the 0-1 cycles/ft range is due to the removal of the 1-2 ft cycle artifacts. Actual frequencies in this range were hidden within the 2 ft artifact pattern and thus were also removed. Unfortunately, the artifact removal suppressed frequencies that likely overlap any evidence for orbital eccentricity: $100 \text{ kyr} * 0.022 \text{ ft/kyr} = 2.2 \text{ ft}$, i.e., a frequency of $1/(2.2 \text{ ft}) = 0.455 \text{ cycles/ft}$.

The inferred PETM to ELMO interval can be compared with the theoretical La2004 astronomical solution for the precession index from 54-56.5 Ma. The amplitude envelope of the theoretical precession index is the orbital eccentricity (e.g., Meyers, 2015). The bandpass filtering of the red intensity in the $f=2$ cycles/ft band allows us to estimate an amplitude envelope using Hilbert transformation that could reveal and be used to reconstruct a record of the orbital eccentricity (**Figure 17**).

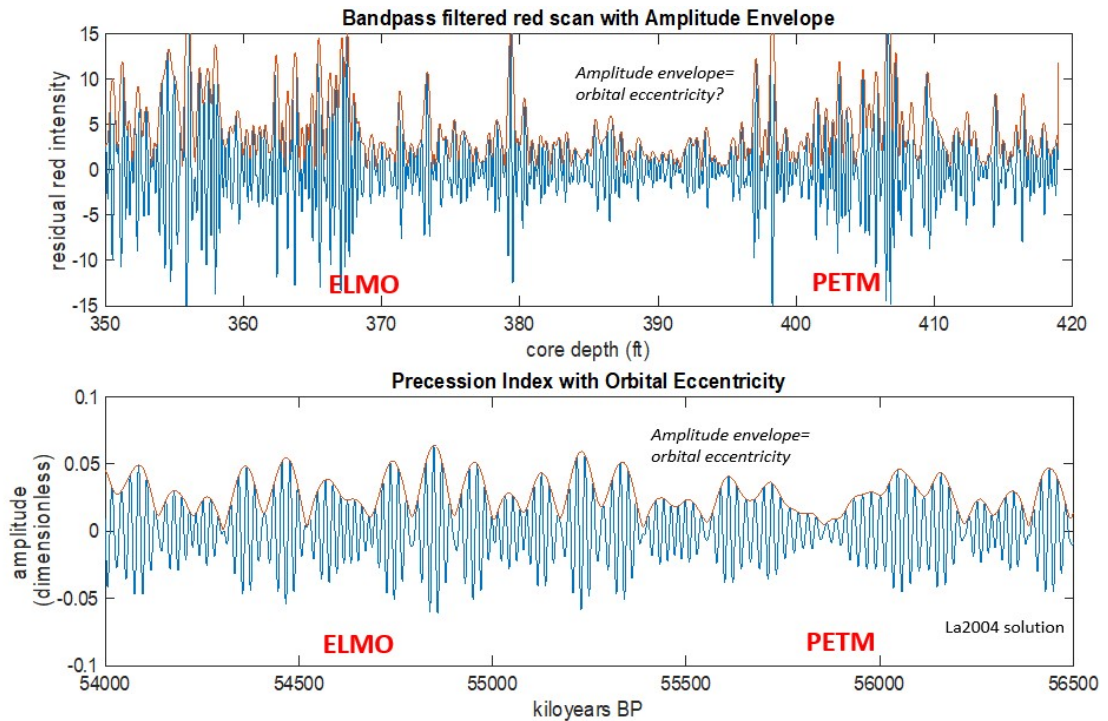
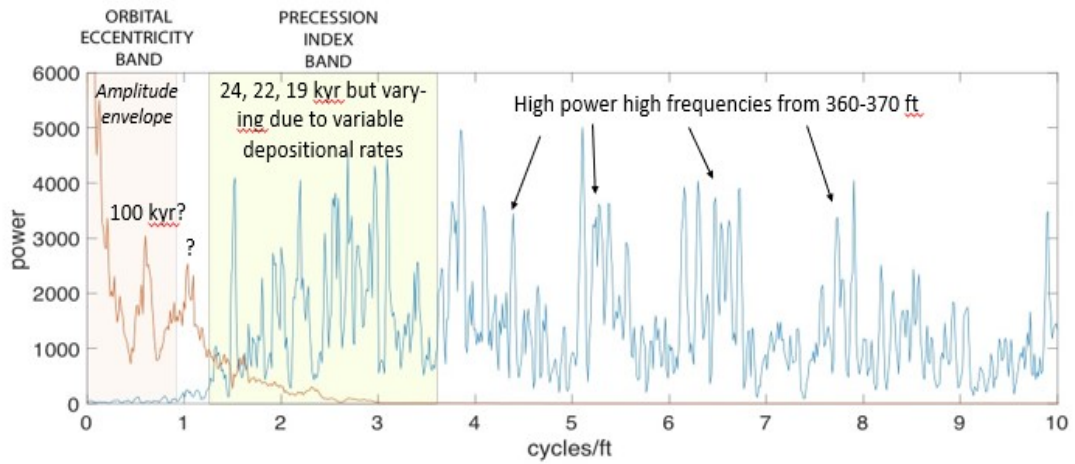


Figure 17: Top: Bandpass-filtered (passband defined in **Figure 15**) power spectrum inverse showing red intensity series (blue), using the Taner filter. Using Hilbert transformation, the amplitude envelope (red) is fitted which represents orbital eccentricity. Bottom: the theoretical model of the Earth's precession index (blue) and orbital eccentricity (red) for 54 Ma to 56.5 Ma. See **Appendix** for MATLAB procedures.

Spectral analysis of the bandpass-filtered amplitude envelope is placed together with the power spectrum of the residual red intensity series, showing reconstructed low frequencies in the 0-2 cycles/ft range, with a prominent peak at $f=0.5$ cycles/ft, which is exactly the frequency predicted to represent 100 kyr (based on the 0.022 ft/kyr sedimentation rate, see above) (**Figure 18**). This result compares favorably with the spectral analysis of the precession index and orbital eccentricity over 54 Ma to 56.5 Ma from the La2004 astronomical solution of Laskar et al. (2004).



2 π MTM Power Spectra of Precession Index and Orbital Eccentricity

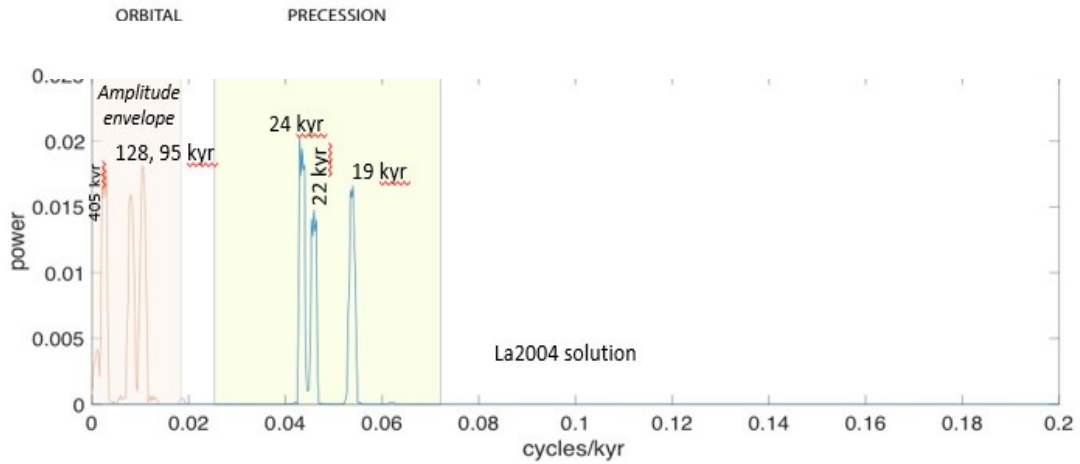


Figure 18: Top: Power spectrum of the residual red intensity series shown in **Figure 17** (blue); power spectrum of the amplitude envelope of the bandpassed residual red intensity series shown in **Figure 15** (red). Bottom: Power spectrum of the La2004 precession index shown in **Figure 17** (blue); power spectrum of the La2004 orbital eccentricity shown in **Figure 17** (red). The high power at frequencies > 3 cycles/ft is from a limited portion of the residual red series, from 360 to 370 ft (see **Section 4.3**).

6. Conclusion

In this thesis, early Eocene hyperthermals including the PETM and ELMO were studied in the Woodland Beach core, Delaware, USA. The main results are as follows:

- The Woodland Beach core is 820 ft long, capturing the Quaternary Delaware Bay Group to Upper Cretaceous Magothy Formation. While multiple drilling gaps are present, other extended intervals were recovered in full.
- The core reveals alternations between sands, silts and clays, glauconitic intervals, shelly or calcareous intervals, and phosphate nodules (near the PETM).
- Core sediment colors range from light or dark brown, dark or light gray, light or dark green-gray, olive-gray, red, orange, and yellow.
- Well logs are continuous but have a low resolution; therefore, the core photographs were scanned for red-green-blue (RGB) intensity.
- The red intensity series of the photographs is analyzed in detail for basic information on oxidizing (high intensity) and reducing (low red intensity) conditions.

- The core photographs have complex lighting artifacts; the red (and green) intensity scans of the individual core sections were analyzed for these artifacts, which typically involved 1-2 ft cycles.
- The PETM to ELMO interval is inferred to be in the Upper Vincentown to Upper Manasquan formations, in the 365 ft to 415 ft interval; no Marlboro Clay is present.
- The PETM-ELMO interval has preserved planktonic and benthonic foraminifera and nannofossils, providing biostratigraphic support.
- Counts of benthonic and planktonic foraminifera from 29 samples taken from 357 ft to 414 ft show a constantly varying ratio that serves as a crude measure of sea level fluctuations and extinction.
- The residual red intensity series for the PETM-ELMO Interval has subtracted these artifacts, and was analyzed further for sedimentary cyclicity.
- The inferred 40 ft PETM-ELMO interval is approximately 1830 kyr long, based on other studies of Milankovitch cycles in deep sea drill cores. This provides an estimated sedimentation rate for the interval of $40 \text{ ft} / (1830 \text{ kyr}) = 0.022 \text{ ft/kyr}$.
- Spectral analysis shows a very “noisy” spectrum due to variable sedimentation rates; the spectrogram reveals evidence for multiple hiatuses.
- The artifact removal suppressed red series frequencies that likely overlap evidence for orbital eccentricity: $\sim 100 \text{ kyr} * 0.022 \text{ ft/kyr} = \sim 2.2 \text{ ft}$.
- If precession index is present in the residual red series, then the orbital eccentricity can be recovered from the precession index amplitude envelope.
- The precession index band of the residual red intensity series was bandpass-filtered and Hilbert-transformed to recover the filter amplitude envelope, and

compared to the La2004 theoretical precession index and orbital eccentricity from 54 Ma to 56.5 Ma.

These findings indicate that the base of the PETM (the Paleocene-Eocene boundary) is located most likely at 407.8 ft in the Woodland Beach core. This conclusion is determined through the absence of benthonic foraminifera at 407 ft, along with five nannofossil identifications. The poor condition of the planktonic foraminifera at 407 ft could be from increased acidity during deposition, another indicator of the PETM onset. The sand percentage is elevated here; its association with glauconite may indicate conditions of low sedimentation. The absence of kaolinite beds (the Marlboro Clay) could be due to the following: there is a long depositional gap in the core; faulting has displaced the Marlboro Clay from the Woodland Beach site; or the site could be at a location within the Salisbury Embayment that did not receive the terrestrial clay influx associated with other PETM Mid-Atlantic cores. Sedimentation rates show 0.459 ft cycles regularly through the red series however, there may be hiatuses, and if cycles are ongoing, unconformities will be difficult to identify unless a 0.459 ft cycle is truncated. The “hiatuses” marked on the spectrogram in **Figure 17** may actually be another artifact caused by the groups of 3 to 5 core sections per photograph, causing an artifact from photograph to photograph (6 to 10 ft long artifacts). Low red intensity values occur at 407.8 ft, suggesting low-oxygen conditions, further supporting the inference for the base of the PETM at this stratigraphic position.

Future work should focus on the following:

- Stable isotope analysis of foraminifera representing the three genera (*Morozovella*, *Acarinina* and *Cibicidoides*) can be undertaken to obtain water depth gradients in $\delta^{13}\text{C}$ and $\delta^{18}\text{O}$ indicating ocean temperature and productivity.
- The remaining half of the core samples can be submitted for organic carbon isotope analysis to more fully characterize the CIE of the PETM.
- The core can be run through a core scanner for high quality imagery with lighting controls to avoid the artifacts that so strongly affect the photographs used in this thesis. This will allow improved characterization of Milankovitch cycles and other sediment variations in the core.

Appendix

MATLAB scripts (% indicate comments)

```
%Converting pixels in ImageJ to depth in feet:
pixels=rgb(:,1);
rgb=RGBProfilesWoodlandBeachNoPicswithblanks;
pixels=rgb(:,1);
figure;plot(rgb(:,2));
dd=820/length(pixels);
depth=0:dd:820;
depth=depth';
depth=depth';
rgbflipped=flipud(rgb);
r=rgbflipped(:,2);
g=rgbflipped(:,3);
b=rgbflipped(:,4);
rminusg=rgbflipped(:,5);
figure;plot(depth,rminusg);
depth=depth-dd;
figure;plot(depth,rminusg);
depth=dd:dd:820;
depth=depth-dd;
depth=depth';
figure;plot(depth,r);
pixels=firsttest(:,1);
rminusg=firsttest(:,5);
testofdepthprofile(:,2)=-1*testofepthprofile(:,2);
testofdepthprofile(:,2)=-1*testofdepthprofile(:,2);
[testdepth,sr]=dephthotime(pixels,testofdepthprofile);
figure;plot(pixels,rminusg);
figure;plot(testdepth,rminusg);
testofdepthprofile(:,2)=-1*testofdepthprofile(:,2);
[testdepth,sr]=dephthotime(pixels,testofdepthprofile);
figure;plot(testdepth,rminusg);
```

```

%Removing artifacts for one segment of core
figure;plot(seg1(:,6),seg1(:,2));
seg1Rsmooth1500L=smooth(seg1(:,2),span,'loess');
hold all; plot(seg1(:,6),seg1Rsmooth1500L);
seg1Rres1500L=seg1(:,2)-seg1Rsmooth1500L;
figure;plot(seg1(:,6),seg1Rres1500L);

%Analysis of R data
% Point MATLAB to redmatthew folder; load "Matthew-Red-Study-in.mat"
%Plot the artifact-processed R dataset
figure;plot(segallRres1500L(:,1),segallRres1500L(:,2));
%flip updown so that depth increases
segallRres1500Lflip=flipud(segallRres1500L);

%analyze the sample rate
diffdR=diff(segallRres1500Lflip(:,1));
figure;plot(diffdR);
%select minimum sample rate for interpolation
ddR=min(diffdR);

% set up interpolated depth scale; segallRres1500Lflip has 100796 points
depthint=segallRres1500Lflip(1,1):ddR:segallRres1500Lflip(100796,1);
depthint=depthint'; %transpose so it is a single column

% interpolate the R values, and plot to check (should look like first plot, above)
segallRres1500Lflipint=interp1(segallRres1500L(:,1),segallRres1500L(:,2),depthint);
figure;plot(depthint, segallRres1500Lflipint);

% calculate power spectrum with multitaper method with default setting (no NW defined);
plot
[p,w]=pmtm(detrend(segallRres1500Lflipint));
f=w/(2*pi*ddR); % convert radial frequency to linear frequency in cycles/ft
figure;plot(f,p); % and limit to f=0,30 cycles/ft range (x-axis)

% store the interpolated dataset into "data" with 2 columns
data=[depthint,segallRres1500Lflipint];

% compute a spectrogram with a running window of 5.0015, step of 0.1; set norm=1
s=evofft(data,5.0015,0.1,ddR,0.,30.,'ft',1);

```

```

%plot with power spectrum, resizing both horizontally
%Resize to be from 385 ft to 415 ft, from 0 to 22 cycles/ft (ticks by 2):
% Filter with passband: fc=2.5, fl=1.0, fh=4.0 cycles/ft; plot
[tanerbandxB, filtout, f]=tanerfilter(segallRres1500Lflipint, ddR, 2.5, 1.0, 4.0);
figure; plot(depthint, tanerbandxB);

%Does it have an amplitude envelope that looks like eccentricity?
[iamp, ifaze, t, ifreq, tm1]=hilbertsignal([depthint, tanerbandxB]);

% Compute MTM power spectrum of instantaneous amplitude series; plot and compare
with original spectrum from f=0 to 10 cycles/ft
[pa, wa]=pmtm(detrend(iamp));
fa=wa/(2*pi*ddR);
figure; plot(fa, pa);

% using complexsignal.m (early version of hilbertsignal.m)
[tc, iampc, ifazec, ufazec, ifreqc] = complexsignal(depthint, ddR, tanerbandxB)

% compute power spectrum of iampc
[pac, wac]=pmtm(detrend(iampc));
fac=wac/(2*pi*ddR);
figure; plot(fac, pac);

```

List of References

Arreguin-Rodriguez, G.J., Thomas, E., D'haenens, S., Speijer, R.P., Alegret, L., 2018. Early Eocene deep-sea benthic foraminiferal faunas: Recovery from the Paleocene Eocene Thermal Maximum extinction in a greenhouse world. *PLoS ONE* 13(2), e0193167.

Bralower, T.J. and Self-Trail, J., 2016. Nannoplankton malformation during the Paleocene-Eocene Thermal Maximum and its paleoecological and paleoceanographic significance. *Paleoceanography*, 31, 1-17.

Bukry, D., 1971. Discoaster evolutionary trends. *Micropaleontology*, 17, 43-52.

Babila, T., Rosenthal, Y., Wright, J., Miller, K., 2016. A continental shelf perspective of ocean acidification and temperature evolution during the Paleocene-Eocene Thermal Maximum. *Geology*, 44, 275-278.

Francus, P., 2007. Image Analysis, Sediments and Paleoenvironments. *Developments in Palaeoenvironmental Research*, 7, Springer, Dordrecht, 330 p.

Hansen J., Sato M., Russell G., Kharecha P., 2013. Climate sensitivity, sea level and atmospheric carbon dioxide. *Philosophical Transactions of the Royal Society, A*, 371, 20120294.

Harris, A.D., Miller, K.G., Browning, J.V., Sugarman, P.J., Olsson, R.K., Cramer, B.S., Wright, J.D., 2010. Integrated stratigraphic studies of Paleocene-lowermost Eocene sequences, New Jersey Coastal Plain: Evidence for glacioeustatic control. *Paleoceanography*, 25, PA3211.

Laskar, J., Robutel, P., Joutel, F., Gasineau, M., Correia, A.C.M., Levrard, B., 2004. A long-term numerical solution for the insolation quantities of the Earth. *Astronomy & Astrophysics*, 428, 261-285.

- Makarova, M., Wright, J.D., Miller, K.G., Babila, T.L., Rosenthal, Y. and Park, J.I., 2016. Hydrographic and ecologic implications of foraminiferal stable isotopic response across the U.S. mid-Atlantic continental shelf during the Paleocene-Eocene Thermal Maximum, *Paleoceanography*, 32, doi:10.1002/2016PA002985.
- McInerney, F.A., and Wing, S.L., 2011. The Paleocene-Eocene Thermal Maximum: A Perturbation of Carbon Cycle, Climate, and Biosphere with Implications for the Future. *Annual Review of Earth and Planetary Sciences*, 39, 489-516.
- Meyers, S.R., 2015. The evaluation of eccentricity-related amplitude modulation and bundling in paleoclimate data: An inverse approach for astrochronologic testing and time scale optimization. *Paleoceanography*, 30, doi:10.1002/2015PA002850
- Miller, K., Browning, J., Mountain, G., Sheridan, R., Sugarman, P., Glenn, S., Christensen, B., 2014. Chapter 3 History of continental shelf and slope sedimentation on the US middle Atlantic margin. *Geological Society, London, Memoirs*, 41, 21-34.
- Miller, K.G., Browning, J.V., Sugarman, P.J., McLaughlin, P.P., Kominz, M.A., Olsson, R.K., Wright, J.D., Cramer, B.S., Pekar, S.J., and Van Sickel, W., 2003. 174AX leg summary: sequences, sea level, tectonics, and aquifer resources: coastal plain drilling. In Miller, K.G., Sugarman, P.J., Browning, J.V., et al., *Proceedings of the Ocean Drilling Program, Initial Reports, 174AX (Supplement): College Station, TX (Ocean Drilling Program)*, 1–38.
- Nederbragt, A.J., and Thurow, J.W., 2007. Digital sediment colour analysis as a method to obtain high resolution climate proxy records, in: Francus, P. (ed)., *Image Analysis, Sediments and Palaeoenvironments. Developments in Palaeoenvironmental Research*, v. 7, Springer, Dordrecht, 105-124.
- Owens, J.P., Bybell, L.M., Paulachok, G., Ager, T.A., Gonzalez, V.M., Sugarman, P.J., 1988. Stratigraphy of the Tertiary Sediments in a 945-foot-deep Corehole near Mays Landing in the Southeastern New Jersey Coastal Plain. U.S. Geological Survey Professional Paper 1484.
- Porrenga, D.H., 1967. Glauconite and Chamosite as Depth Indicators in the Marine Environment. *Marine Geology*, 5, 495-501.
- Self-Trail, J.M., Robinson, M.M., Bralower, T.J., Sessa, J.A., Hajek, E.A., Kump, L.R., Trampush, S.M., Willard, D.A., Edwards, L.E., Powars, D.S., Wandless, G.A., 2017. Shallow marine response to global climate change during the Paleocene-Eocene Thermal Maximum, Salisbury Embayment, USA. *Paleoceanography*, 32, 710-728.

Sluijs, A., Schouten, S., Pagani, M., Woltering, M., Brinkhuis, H., Sinninghe Damsté, J.S., Dickens, G.R., Huber, M., Reichert, G.J., Stein, R., Matthiessen, J., Lourens, L.J., Pedentchouk, N., Backman, J., Moran, K., Expedition 302 Scientists, 2006. Subtropical Arctic Ocean temperatures during the Palaeocene–Eocene Thermal Maximum. *Nature*, 441, 610–613.

Stassen, P., Thomas, E., Speijer, R.P., 2012. Integrated stratigraphy of the Paleocene–Eocene thermal maximum in the New Jersey Coastal Plain: Toward understanding the effects of global warming in a shelf environment. *Paleoceanography and Paleoclimatology* 27, PA4210.

Vandenbergh, N., Hilgen, F.J., Speijer, R.P., 2012. Chapter 28 – The Paleogene Period. In: Gradstein, F.M., Ogg, J.G., Schmitz, M. and Ogg, G.G. (eds.), *The Geologic Time Scale 2012*, Elsevier, 855-921.

Ward, L.W., Powars, D.S., 2014. Tertiary Lithology and Paleontology, Chesapeake Bay Region. *Geology of the National Capital Region-Field Trip Guidebook*, 263-298.

Westerhold, T., Rohl, U., Laskar, J., Raffi, I., Bowles, J., Lourens, L.J., Zachos, J.C., 2007. On the duration of magnetochrons C24r and C25n and the timing of early Eocene global warming events: Implications from the Ocean Drilling Program Leg 208 Walvis Ridge depth transect. *Paleoceanography*, 22.

Westerhold, T., Rohl, U., Wilkens, R.H., Gingerich, P.D., Clyde, W.C., Wing, S.L., Bowen, G.J., Kraus, M.J., 2018. Synchronizing early Eocene deep-sea and continental records – cyclostratigraphic age models for the Bighorn Basin Coring Project drill cores. *Climate of the Past* 14, 303-319.

Zachos, J.C., McCarren, H., Murphy, B., Rohl, U., Westerhold, T., 2010. Tempo and scale of late Paleocene and early Eocene carbon isotope cycles: Implications for the origin of hyperthermals. *Earth and Planetary Science Letters*, 299, 242-249.

Zachos, J.C., Schouten, S., Bohaty, S., Quattlebaum, T., Sluijs, A., Brinkhuis, H., Gibbs, S., Bralower, T., 2006. Extreme warming of the mid-latitude coastal ocean during the Paleocene–Eocene Thermal Maximum: inferences from TEX86 and isotope data. *Geology*, 34, 737–740.

Biography

Matthew Smith received his Bachelor of Science in Geology at Louisiana State University in 2014. He graduated from Rutherford Highschool's International Baccalaureate program. He has worked as a mudlogger in Oklahoma, had internships in government and private geology/environmental programs, and as a camp counselor in Vermont. After graduation, he hopes to work on research involving changes to the water table of his home town of Panama City, Florida post Hurricane Michael.